Journal of Biomechanics 41 (2008) 3085–3089

Contents lists available at ScienceDirect

Journal of Biomechanics

journal homepage: www.elsevier.com/locate/jbiomech
www.JBiomech.com

Short communication

A comparison of seven methods of within-subjects rigid-body pedobarographic image registration

Todd C. Pataky [a,*], John Y. Goulermas [b], Robin H. Crompton [a]

[a] HACB, School of Biomedical Sciences, University of Liverpool, Sherrington Buildings, Ashton Street, Liverpool L69 3GE, UK
[b] Department of Electrical Engineering and Electronics, University of Liverpool, UK

ARTICLE INFO

Article history:
Accepted 5 August 2008

Keywords:
Plantar pressure measurement
Human foot
Biomedical image processing
Gait biomechanics
Locomotion

ABSTRACT

Image registration, the process of transforming images such that homologous structures optimally overlap, provides the pre-processing foundation for pixel-level functional image analysis. The purpose of this study was to compare the performances of seven methods of within-subjects pedobarographic image registration: (1) manual, (2) principal axes, (3) centre of pressure trajectory, (4) mean squared error, (5) probability-weighted variance, (6) mutual information, and (7) exclusive OR. We assumed that foot-contact geometry changes were negligibly small trial-to-trial and thus that a rigid-body transformation could yield optimum registration performance. Thirty image pairs were randomly selected from our laboratory database and were registered using each method. To compensate for inter-rater variability, the mean registration parameters across 10 raters were taken as representative of manual registration. Registration performance was assessed using four dissimilarity metrics (#4–7 above). One-way MANOVA found significant differences between the methods ($p<0.001$). Bonferroni post-hoc tests revealed that the centre of pressure method performed the poorest ($p<0.001$) and that the principal axes method tended to perform more poorly than remaining methods ($p<0.070$). Average manual registration was not different from the remaining methods ($p = 1.000$). The results suggest that a variety of linear registration methods are appropriate for within-subjects pedobarographic images, and that manual image registration is a viable alternative to algorithmic registration when parameters are averaged across raters. The latter finding, in particular, may be useful for cases of image peculiarities resulting from outlier trials or from experimental manipulations that induce substantial changes in contact area or pressure profile geometry.

1. Introduction

Image registration refers to the process of transforming one image, termed a 'source', to match a second image, termed a 'template', such that homologous structures optimally overlap. Performed routinely in many diverse imaging domains (Goshtasby, 2005), registration is necessary for the pixel-level statistical comparison of functional images (Ashburner and Friston, 2007). There are a plethora of registration techniques in medical imaging alone (Maintz and Viergever, 1998), indicating that optimal algorithms are largely problem dependent.

Registration has been conducted previously in pedobarography using principal axis (PA) transformations (Harrison and Hillard, 2000), finite element-based modal matching (Tavares et al., 2000; Bastos and Tavares, 2004; Pinho and Tavares, 2004), and optimal linear transformations (Pataky and Goulermas, 2008), but these techniques represent a small subset of those described in the general image registration literature (Brown, 1992; Maintz and Viergever, 1998; Zitova and Flusser, 2003). Recent demonstration of both the statistical and biomechanical benefits of registration-supported pedobarographic analysis (Pataky et al., 2008) has emphasized the importance of registration in pedobarography and has created the need for scrutiny of pedobarographic image registration procedures.

The purposes of this study were: (1) to quantitatively compare the performance of a variety of rigid-body pedobarographic image registration techniques and (2) to assess whether manual registration is a viable alternative to algorithmic registration. We limit current analyses to rigid-body transformations because they are the simplest type of image transformation and have previously yielded successful within-subject results in pedobarography (Pataky and Goulermas, 2008). Potential limitations are discussed.

2. Methods

2.1. Images

Thirty peak pressure template-source pairs were analysed. Three image pairs were selected randomly for each of 10 random subjects (four females, six males;

* Corresponding author. Tel.: +44 151 794 5500.
E-mail address: tpataky@liv.ac.uk (T.C. Pataky).

0021-9290/$ - see front matter © 2008 Elsevier Ltd. All rights reserved.
doi:10.1016/j.jbiomech.2008.08.001

age: 30.1±7.4 years) from our database of 47 healthy subjects. Each subject had performed at least 10 self-paced walking trials over a 10 m gait runway. Pedobarographic data were originally collected at 500 Hz using a 0.5 m Footscan 3D system (RSscan, Olen, Belgium). Prior to participation both subjects and raters (Section 2.2.1) gave informed consent according to the policies of the Research Ethics Committee of the University of Liverpool.

Images were vertically stretched by a factor of 1.5 to correct for non-square sensor array spacing (5.08 × 7.62 mm/sensor, manufacturer specified). Image transformations were performed (here and throughout) using bilinear interpolation resampling (Goshtasby, 2005, pp. 145–146). Images were then spatially smoothed using convolution filtering and morphological opening (Pataky and Goulermas, 2008). All image processing was conducted using MATLAB 7.4 (The MathWorks, USA).

2.2. Registration methods

2.2.1. Manual (MAN)

Ten raters (age: 25.0±5.4 years) manually registered images using a laptop keyboard (Fig. 1). Raters had no prior image registration experience. All participated in a 5 min programmed tutorial/training session prior to experimentation. Since single registration trials are not accurate (Flynn et al., 1999), raters performed five repetitions of each image in a fully randomized order. The mean rigid-body transformation parameters $\boldsymbol{q}$ (Eq. (1)) were taken as representative of this technique:

$$\boldsymbol{q} = [q_1 \quad q_2 \quad q_3] = \frac{1}{50}\sum_{i=1}^{10}\sum_{j=1}^{5}[x_{ij} \quad y_{ij} \quad \theta_{ij}] \tag{1}$$

where i and j index raters and repetitions, respectively; x, y, and θ are horizontal translation, vertical translation, and rotation, respectively.

2.2.2. Principal axes (PA)

Following Harrison and Hillard (2000), PA were computed as the eigenvectors of the pressure-weighted covariance matrix $\boldsymbol{M}$:

$$\boldsymbol{M} = \sum_k I_k(\boldsymbol{r}_k - \boldsymbol{c})(\boldsymbol{r}_k - \boldsymbol{c})^{\mathrm{T}} \tag{2}$$

where I_k is the pressure at the kth pixel, and where $\boldsymbol{r}_k$ and $\boldsymbol{c}$ are column vectors representing peak pressure image pixel position and centroid (Eq. (3)), respectively. The source image was transformed so that its centroid and PA were coincident with those of the template.

2.2.3. Centre of pressure trajectory (COP)

The COP trajectory $\boldsymbol{c}(t)$ was calculated as the path of the instantaneous centroid (at time t):

$$\boldsymbol{c}(t) = \frac{\sum I_k(t)\boldsymbol{r}_k}{\sum I_k(t)} \tag{3}$$

The sum of the squared error between the COP trajectories of an image pair was then minimized.

2.2.4. Mean squared error (MSE)

MSE was calculated over non-zero pixels:

$$f_{\mathrm{MSE}} = \frac{1}{N}\sum_k (I_{0k} - I_{1k})^2 \tag{4}$$

where N is the total number of non-zero pixels in the mean image; I_0 and I_1 are the template and source image, respectively. The symbol 'f' is used here and for the remainder of registration methods to highlight that these functions were used as (dis)similarity metrics to quantify registration performance.

2.2.5. Probability-weighted variance (VAR)

Following Flynn et al. (1999):

$$f_{\mathrm{VAR}} = \frac{1}{X}\sum_x p_0(x)\sigma_1(x) \tag{5}$$

where $p_0(x)$ is the probability that a pixel in the template image has a value of x, and where $\sigma_1(x)$ is the standard deviation of the pressure values of the corresponding source pixels. We used $X = 20$ discrete bins. The idea is that locations which have similar pressure in the template should have minimum variance in the source.

2.2.6. Mutual information (MI)

MI was computed as:

$$f_{\mathrm{MI}} = H(I_0) + H(I_1) - H(I_0, I_1)$$
$$H(I) = -\sum_x p(x)\log p(x) \tag{6}$$

where $H(I)$ is the Shannon entropy of the pixels in image I and where $H(I_0,I_1)$ is the joint entropy (Pluim et al., 2003). We used 20 discrete bins (as above) for probability estimates.

2.2.7. Exclusive or (XOR)

Following Pataky and Goulermas (2008):

$$f_{\mathrm{XOR}} = \frac{|I_0 \oplus I_1|}{|I_0| + |I_1|} \times 100\% \tag{7}$$

where I_0 and I_1 are binary template and source images, respectively, defined by the inequality: $(I>0)$. The symbol '$\oplus$' is the 'exclusive or' set operator and the vertical bars indicate set size. This function maximizes overlap by minimizing the number of non-zero pixels that are either in the template or source, but not in both.

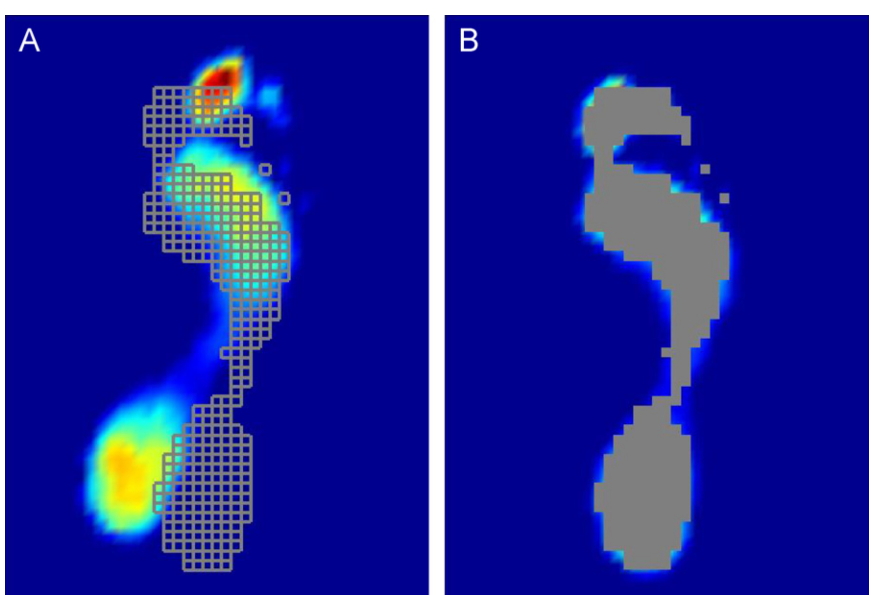

Fig. 1. Manual registration screenshots: (A) before and (B) after registration. The source was rendered using linear nodal interpolation and the template was rendered either as an array of empty grey squares (A) or as a solid grey shape (B). Users could toggle between these template states using the spacebar to facilitate registration perception. The arrow keys and the square bracket keys were used to translate and rotate the source in increments of 0.1 pixels (= 0.508 mm) and 0.1°, respectively.